NIH Public Access
Author Manuscript
Dev Biol. Author manuscript; available in PMC 2011 November 15.

Published in final edited form as:
Dev Biol. 2010 November 15; 347(2): 369–381. doi:10.1016/j.ydbio.2010.09.002.

BMP/SMAD Signaling Regulates the Cell Behaviors that Drive the Initial Dorsal-Specific Regional Morphogenesis of the Otocyst

Sho Ohta[1], **Suzanne L. Mansour**[2], and **Gary C. Schoenwolf**[1]

[1]Department of Neurobiology and Anatomy, University of Utah School of Medicine, Salt Lake City, Utah, USA

[2]Department of Human Genetics, University of Utah School of Medicine, Salt Lake City, Utah, USA

SUMMARY

During development of the otocyst, regional morphogenesis establishes a dorsal vestibular chamber and a ventral auditory chamber, which collectively constitute the membranous labyrinth of the inner ear. We identified the earliest morphogenetic event heralding the formation of the vestibular chamber, a rapid thinning and expansion of the dorsolateral wall of the otocyst, and showed that this process is generated by changes in otocyst cell shape from columnar to squamous, as opposed to changes in other cell behaviors, such as localized changes in cell proliferation or cell death. Moreover, we showed that thinning and expansion of the dorsolateral otocyst is regulated by BMP/SMAD signaling, which is both sufficient and necessary for localized thinning and expansion. Finally, we showed that BMP/SMAD signaling causes fragmentation of E-cadherin in the dorsolateral otocyst, occurring concomitantly with cell-shape change, suggesting that BMP/SMAD signaling regulates cell-cell adhesion during the initial morphogenesis of the otocyst epithelium. Collectively, our results show that BMP signaling via SMADs regulates the cell behaviors that drive the initial dorsal-specific morphogenesis of the otocyst, providing new information about how regional morphogenesis of a complex organ rudiment, the developing membranous labyrinth, is initiated.

Keywords

Inner ear; otic vesicle; patterning; BMP; SMAD; E-cadherin

INTRODUCTION

The developing inner ear provides a unique system in which to analyze the morphogenetic events that transform a simple epithelial embryonic rudiment—the otocyst—into an elaborate three-dimensional, functional organ—the membranous labyrinth. The origin of the inner ear is simple: it arises from the otic placode, a plate-like region of thickened epithelial

© 2010 Elsevier Inc. All rights reserved.

Author for Correspondence: Gary C. Schoenwolf, Ph.D., Department of Neurobiology and Anatomy, University of Utah School of Medicine, 30 N. 1900 E., Room 2R066, Salt Lake City, Utah, 84132-3401, Schoenwolf@neuro.utah.edu, Phone: 801-581-6453, Fax: 801-581-8852.

Publisher's Disclaimer: This is a PDF file of an unedited manuscript that has been accepted for publication. As a service to our customers we are providing this early version of the manuscript. The manuscript will undergo copyediting, typesetting, and review of the resulting proof before it is published in its final citable form. Please note that during the production process errors may be discovered which could affect the content, and all legal disclaimers that apply to the journal pertain.

NIH-PA Author Manuscript
NIH-PA Author Manuscript
NIH-PA Author Manuscript

NIH-PA Author Manuscript

NIH-PA Author Manuscript

NIH-PA Author Manuscript

cells adjacent to the hindbrain, which subsequently invaginates and pinches off from the overlying ectoderm to form a hollow epithelial structure called the otocyst or otic vesicle. In turn, the otocyst gives rise to the membranous labyrinth through regional morphogenesis, a process is which the otocyst is sculpted into a dorsal vestibular chamber, responsible for the perception of motion and body position, and a ventral auditory chamber, responsible for the perception of sound (reviewed by Barald and Kelley, 2004; Mansour and Schoenwolf, 2005; Bok et al., 2007a; Ohyama et al., 2007; Whitfield and Hammond, 2007; Ladher et al., 2010).

Three lines of evidence strongly suggest that stereotypic morphogenesis of the membranous labyrinth is essential for establishing normal auditory and vestibular function—that is, that both form and function are critically *inter*dependent. First, in as many as 30–40% of children with sensorineural hearing loss, imaging reveals significant inner ear malformations (Antonelli et al., 1999; Purcell et al., 2003). For example, in one population of patients with sensorineural hearing loss, inner ear malformations were observed in 38% of the cases, typically including enlarged vestibular aqueduct, Mondini dysplasia, large vestibule, and semicircular canal dysplasia (Wu et al., 2005). Similarly, enlarged vestibular aqueduct has been correlated with vestibular symptoms in children (Grimmer and Hedlund, 2007; Worden and Blevins, 2007), although whether this anomaly represents a defect in morphogenesis or a post-morphogenesis enlargement is unclear. Second, in animal models, experimentally induced changes in otocyst morphogenesis similar to those seen in patients can compromise inner ear function, even when hair and supporting cells are generated (e.g., Hatch et al., 2007; Nichols et al., 2008; Koo et al., 2009). Third, theoretical modeling supported by analytical studies (Manoussaki et al., 2008) demonstrates that cochlear shape is correlated with the cochlea's response to low frequencies, emphasizing the importance of proper cochlear morphogenesis in hearing.

Our understanding of the cellular and molecular mechanisms underlying regional morphogenesis of the otocyst is highly limited. Formation of the vestibular chamber is complex and involves several morphogenetic events, including initial dorsolateral outgrowth of a primordial canal pouch that is remodeled into the anterior and posterior semicircular canals, followed by lateral outgrowth of a second canal pouch that is remodeled into the lateral semicircular canal (Chang et al., 1999; 2004a). Only the remodeling stage of vestibular chamber morphogenesis has been analyzed at the level of cell behaviors: it involves focal apoptosis in the chick and Xenopus (Haddon and Lewis, 1991; Fekete et al., 1997), and cell rearrangements in the mouse (Martin and Swenson, 1993). Formation of the auditory chamber involves the ventromedial outgrowth of the otocyst wall to form the cochlear bud, and the rapid elongation of this bud to form the cochlear duct (Bissonnette and Fekete, 1996; Morsli et al., 1998). The cell behaviors driving the latter event are better understood and include a mediolateral cell-cell intercalation that results in a convergent extension movement, which concomitantly narrows and lengthens the duct as cells merge toward the center (Yamamoto et al., 2009).

Not only is our understanding of the cell behaviors that drive regional morphogenesis of the otocyst limited, so are the signaling pathways that directly control the particular cell behaviors driving morphogenesis. Several signaling pathways regulate development of the vestibular and auditory chambers of the inner ear, including the WNT (Dabdoub et al., 2003; Montcouquiol and Kelley, 2003; Montcouquiol et al., 2003, 2006; Dabdoub and Kelley, 2005; Riccomagno et al., 2005; Wang et al., 2005; Kelly and Chen, 2007; Qian et al., 2007; Rida and Chen, 2009; Yamamoto et al., 2009), BMP (Chang et al., 1999, 2002, 2004b, 2008; Gerlach et al., 2000; Bok et al., 2007b; Hammond et al., 2009; Hwang et al., 2010), SHH (Riccomagno et al., 2002, 2005; Bok et al., 2007c; Hammond et al., 2010; Sapède and Pujades, 2010), and FGF (Mansour et al., 1993; Léger and Brand, 2002; Pauley et al., 2003; Ohuchi et al., 2005; Hatch et al., 2007; Zelarayan et al., 2007) pathways. However, in only

NIH-PA Author Manuscript

NIH-PA Author Manuscript

NIH-PA Author Manuscript

one case do we know the cell behaviors directly regulated by signaling: namely, non-canonical WNT signaling controls cell-cell intercalation and convergent extension in the elongating cochlear duct (Dabdoub et al., 2003; Dabdoub and Kelley, 2005; Kelly and Chen, 2007; Rida and Chen, 2009).

In this study, we examined the molecular signaling regulating the initial morphogenetic event heralding formation of the vestibular chamber: rapid thinning and expansion of the dorsolateral wall of the otocyst to form the primordial canal outpouch. We show that thinning and expansion is driven by changes in otocyst cell shape from columnar to squamous, and not by other cell behaviors such as localized cell proliferation or death, and that change in cell shape is accompanied by E-cadherin fragmentation, suggesting that changes in cell-cell adhesion are required for this morphogenesis to occur. We further show that BMP signaling, acting through SMADs, is both sufficient and necessary for thinning and expansion. In summary, our studies demonstrate an essential role for BMP signaling in initiating regional morphogenesis of the dorsal otocyst to form the vestibular chamber of the inner ear.

MATERIALS AND METHODS

Embryos

Fertilized White Leghorn chicken eggs were purchased from Merrill's Poultry Farm (Idaho, USA). Eggs were incubated at 38.5°C and staged according to the criteria of Hamburger and Hamilton (1951; HH; reprinted as Hamburger and Hamilton, 1992). CD-1 (Charles River) mice were mated to obtain embryos at desired stages, indicated as embryonic (E) days following detection of a vaginal plug. All animal studies complied with protocols approved by the University of Utah Institutional Animal Care and Use Committee.

In situ hybridization for gene expression analysis

Whole-mount in situ hybridization was performed using standard procedures with chicken (c) probes for *Bmp2*, *Bmp4*, *Bmp7*, and *Smad6* (kindly provided by T. Nohno, Kawasaki Medical School, Okayama, Japan; C. Tickle, University of Dundee, UK; B. Houston, University of Dundee, UK; and E. Laufer, Columbia University, USA). In a subset of embryos, the otocyst was first opened with a tungsten needle to avoid trapping of probes and detection reagents.

Chick *Bmp* type-1 and type-2 receptor probes were obtained by RT-PCR using the following primers:

BmpRIA: 5'-AGCGATTGCTTGGAGCCTATCT-3' and 5'-AGCTGGCTTCTTCTGTGGTGAA-3'

BmpRIB: 5'-GACACTCCTATTCCACACCA-3' and 5'-GAGCTTAATGTCCTGCGACT-3'

BmpRII: 5'-GGTCGATACGGAGCAGTGTACA-3' and 5'-CTGCTCCTTCAAGCACTTCTGG-3'

Mouse (m) *Bmp* type-1 and type-2 receptors were obtained by RT-PCR using the following primers:

BmpRIA: 5'-GTGAGCATCAAGTGGCATTGG-3' and 5'-GACACAAGAGAAGAGGGGAGAGTCG-3'

BmpRIB: 5'-AAAGCATCCCTCTGTGTTTCACTC-3' and 5'-CCAAGGACGCTTTTTGCCCCTCTT-3'

NIH-PA Author Manuscript

NIH-PA Author Manuscript

NIH-PA Author Manuscript

BmpRII: 5'-AACCACCACAAACACCACCG-3' and 5'-GATACTTACCACACCGTCCATCTTC-3'

Immunohistochemistry

Paraffin sections of chick and mouse embryos fixed with 4% paraformaldehyde (PFA) were prepared with a microtome (Leica LM2255) and either stained with hematoxylin and/or eosin or subjected to immunostaining using standard procedures. For immunohistochemistry, specimens were incubated at a 1:100 dilution in PBST (phosphate-buffered saline plus 0.1% Tween20) containing 0.2% fetal bovine serum (FBS) either for 2 hours at room temperature or overnight at 4°C with the following primary antibodies: anti-GFP (mouse monoclonal, Roche, Cat. #11814460001), anti-E-cadherin (mouse monoclonal, BD Bioscience, Cat. #610182), anti-pSMAD1/5/8 (rabbit polyclonal, Cell Signaling Technology, Cat. #9511), and anti-laminin (rabbit polyclonal, SIGMA, Cat. #L9393). After three washes with PBST, specimens were incubated with the following secondary antibodies diluted 1:200 in a solution of PBST containing 0.2% FBS: Alexa Fluor 488 goat anti-mouse IgG or Alexa Fluor 594 goat anti-rabbit IgG (Molecular Probes). In many cases, sections were then counterstained with Hoechst stain to mark cell nuclei.

Terminal dUTP Nuclear End Labeling (TUNEL) was done according to the manufacturer's procedures (In Situ Cell Death Detection Kit, Fluorescein: Cat. #11684795910, Roche). Sections were counterstained with Hoechst stain.

5-ethynyl-2'-deoxyuridine (EdU) labeling was done according to the procedure described by Warren and co-workers (Warren et al., 2009). Chick eggs were windowed, the vitelline membranes were opened, and 100–200 µl of 500 µM EdU in 0.9% NaCl was added onto the underlying embryos. After 2 or 24 hours of incubation, embryos were harvested and fixed in 4% PFA for 1–2 hours at 4°C. EdU labeling was detected following the manufacturer's procedures (Click-iT® EdU Alexa Fluor® 488 Imaging Kit for 50 coverslips: Cat. #C10337, Invitrogen). In addition, cell embryos were labeled with an antibody to phosphorylated Histone H3 (pHH3: rabbit polyclonal, Upstate Biotechnology, Inc., Cat. #06570), as a second means to assess cell division.

In ovo sonoporation

HH 11–14 chick embryos were sonoporated in ovo. To prepare the DNA-microbubble mixture, 10 µl of a plasmid DNA solution (concentration 2.0–4.0 µg/µl), (pCAGGS-GFP, pCAGGS-m*Noggin*, or pCAGGS-m*Bmp4*; the GFP vector was co-sonoporated with the gene of interest), was added to 10 µl of SonoVue (BRACCO, Milan, Italy, purchased from Protech, Texas, USA). Eggs were windowed, the vitelline and amniotic membranes were opened, and the DNA-microbubble mixture was injected into the head mesenchyme adjacent to the otocyst using a glass micropipette (GD-1.2: Narishige, Tokyo, Japan). Injected chick embryos were immediately exposed to ultrasound using a 3-mm diameter ultrasound probe (Sonitron 2000N, Rich-Mar, Inola, OK, purchased from Nepagene) with a frequency of 1 MHz, an intensity of 2.0 W/cm2, and a pulse-duty ratio of 20% for a duration of 60 seconds.

In ovo electroporation

HH 15–16 chick embryos were electroporated in ovo. Eggs were windowed, the vitelline and amniotic membranes were opened, and the plasmid solution—2.0 µg/µl of pCAGGS-GFP and pCS2-h*Smad6* (Addgene plasmid no. 14960) plus 0.1% Fast Green to enable visualization of the injected site—was injected into the cavity of the right otocyst (upper following torsion of the head) with a fine glass micropipette. Positive and negative electrodes were placed lateral to the right otocyst and beneath the neural tube, respectively. Two 50-millisecond pulses at 10 volts were applied using a CUY21 electroporator.

NIH-PA Author Manuscript

NIH-PA Author Manuscript

NIH-PA Author Manuscript

Dorsomorphin treatment

HH 14–16 chick embryos were treated with Dorsomorphin. A 10 mM stock of Dorsomorphin (CALBIOCHEM, Merck, Darmstadt, Germany, Cat. #171261) in DMSO was diluted to a working concentration of 50 μM in PBS. After windowing eggs and opening of the vitelline and amniotic membranes over the desired site, 100 μl of 50 μM Dorsomorphin or vehicle alone was dropped onto the embryo. Because of torsion of the head, and the well-like space created between the yolk and the left side of the head after breeching of the amnion, only the left otocyst facing the yolk sac was soaked in Dorsomorphin or vehicle, with the right (upper otocyst) serving as an internal control.

Imaging and 3D reconstruction

The otocyst, together with surrounding mesenchyme and adjacent hindbrain, was dissected from the embryo using forceps and microscissors. Dissected tissues were then treated with 0.1 mg/ml of collagenase A (Roche) in Hanks balanced salt solution (HBSS) at 37°C for 20 minutes, and otocysts were isolated using sharp tungsten needles and placed in 4% PFA for 2 hours at 4°C. Immunostaining of intact isolated otocysts was done as described above and specimens were cleared with a glycerol series.

Serial confocal optical sections at 0.62 μm intervals were taken with an FV-1000 confocal microscope (Olympus) and a water-immersion 40x objective (0.75 numerical aperture). Optical sections were collected from the dorsolateral side of the chick otocyst. Alexa Fluor 488 or GFP was excited with a 488 nm laser, and Alexa Fluor 594 was excited with a 560 nm laser. The confocal dataset was subjected to 3D reconstruction using Osirix imaging software (http://www.osirix-viewer.com) or Amira software (Visage Imaging™, San Diego, CA). The size, contrast, and brightness of the resulting images were adjusted with Photoshop CS3 (Adobe Systems, San Jose, CA) and Image J 1.38x (NIH, USA).

In addition, paraffin serial transverse sections of mouse embryos at E9.5, 10.5, and 11.5 were photographed and the otocysts were reconstructed in three dimensions using Amira software.

RESULTS

The dorsolateral wall of the otocyst undergoes rapid thinning and expansion, driven by cell-shape changes, to form the primordial canal outpouch, presaging formation of the vestibular chamber

During development of the inner ear, the ectoderm flanking the caudal hindbrain is induced by adjacent tissues to thicken as the otic placode, which rapidly invaginates to form the otic pit or cup. In turn, the otic cup pinches off from the overlying ectoderm to form the fluid-filled otic vesicle or otocyst (Barald and Kelley, 2004; Mansour and Schoenwolf, 2005; Bok et al., 2007a; Ohyama et al., 2007; Whitfield and Hammond, 2007; Ladher et al., 2010; Fig. 1A, B: HH 16).

We used confocal microscopy to three-dimensionally reconstruct E-cadherin-labeled chick otocysts at HH 16–20 and observed that the dorsolateral wall of the otocyst (hereafter called dorsolateral otocyst) expanded rapidly along its anterior-posterior axis to form the primordial canal outpouch, the initial rudiment of the vestibular chamber (Fig. 1A; asterisks, HH 16: n = 5; HH 18: n = 5; HH 20: n = 8). This expansion was even more evident in serial transverse sections, which also revealed that expansion was accompanied by thinning of the epithelium (Fig. 1B–D, HH 16: n = 8; HH 18: n = 10; HH 20: n = 12). Examination of transverse sections at higher magnification showed that the wall of the early otocyst (HH 16) consisted of a pseudostratified columnar epithelium containing multiple (3–4) nuclear layers

NIH-PA Author Manuscript

NIH-PA Author Manuscript

NIH-PA Author Manuscript

(Fig. 1B'). As epithelial thinning and expansion occurred, the dorsolateral otocyst cells transformed their shape to cuboidal, by HH 18 (Fig. 1C'), and squamous, by HH 20 (Fig. 1D'), such that the dorsolateral epithelium became flattened, consisting of a single nuclear layer. Thus, expansion of the dorsolateral epithelium involved a concomitant and dramatic change in cell shape.

To better characterize cell-shape changes, we electroporated cells within the dorsolateral otocyst during its thinning and expansion with a cytoplasmic GFP-expression vector, and counterstained their nuclei with Hoechst stain. Confocal microscopy was used to reconstruct cell shapes and determine cell dimensions. To do this, ten cells were selected for measurement at each time point from a total of nine transfected embryos. Although more than 100 cells were labeled in these embryos after transfection, only a small subset of cells could be reconstructed because cell boundaries could not be easily distinguished when two or more adjacent cells were GFP-labeled, so only isolated transfected cells could be used. The apicobasal height of the reconstructed cells was determined by adding the total number of optical sections that passed through each cell times their Z value. The maximal width of each cell was measured in an optical section at the level of the mid-apicobasal plane of its nucleus. Individual cells in the dorsolateral otocyst became approximately one-third shorter and three-fold wider during epithelial thinning and expansion between HH 16 and HH 24 (Fig. 1E), providing direct evidence that individual cells in the dorsolateral otocyst change their shape from columnar to squamous during rapid thinning and expansion.

To determine whether thinning and expansion of the dorsolateral otocyst was unique to the chick otocyst or a more universal event of otocyst development in higher vertebrates, we examined serial sections of the embryonic mouse otocyst at E9.5–11.5 (Suppl. Fig. 1A–C) and generated 3-D reconstructions (Suppl. Fig. 1A'–C'). Thinning and expansion of the dorsolateral otocyst also occurred in the mouse, suggesting that this regional morphogenetic event is characteristic of early otocyst development in amniotes.

Increased cell proliferation does not play a major role in driving expansion of the dorsolateral otocyst

In addition to cell-shape changes, increases in cell number resulting from increased proliferation could also cause epithelial expansion (e.g., during branching morphogenesis of a variety of organs: reviewed by Affolter et al., 2009; Andrew and Ewald, 2010). To address this possibility, we labeled mitotic cells in the otocyst either using antibodies directed against phosphorylated Histone H3 (pHH3) or by pulsing embryos for 2 hours with EdU. Similar results were obtained with the two approaches, so discussion of only the EdU results is presented. At HH 16, a locus of reduced cell proliferation was observed in the region of the dorsolateral otocyst as described previously (Fig. 2A; n = 4; Lang et al., 2000). Furthermore, TUNEL-positive cells were also detected at this same region of reduced cell proliferation in association with closure of the otic cup into the otic vesicle (data not shown), thus confirming the previous report of Lang and co-workers (Lang et al., 2000). At HH 18–20, stages at which the dorsolateral otocyst is undergoing rapid thinning and expansion, few EdU-positive cells were detected in the dorsolateral otocyst, whereas the ventral otocyst showed robust cell proliferation (Fig. 2B; HH 18: n = 4; HH 20: n = 4), again confirming the previous report of Lang and co-workers (Lang et al., 2000). At these stages TUNEL-positive cells were no longer observed at the dorsolateral otocyst, but were detected in the otic epithelium near the forming statoacoustic ganglion (data not shown), again confirming the previous report of Lang and co-workers (Lang et al., 2000). These data suggest that proliferation and programmed cell death do not play a major role in driving thinning and expansion of the dorsolateral otocyst, further suggesting that cell-shape change from columnar to squamous provides the major driving force for localized epithelial expansion.

NIH-PA Author Manuscript

NIH-PA Author Manuscript

NIH-PA Author Manuscript

Cell-shape change in the dorsolateral otocyst is accompanied by changes in E-cadherin distribution

The shape of epithelial cells within a cell sheet is influenced by the distribution of adherens junctions and associated cell adhesion molecules such as E-cadherin (reviewed by Carthew, 2005). Thus, changes in the configurations of cells during epithelial morphogenesis, such as those occurring during thinning and expansion of the dorsolateral otocyst, are expected to be accompanied by changes in the distribution of cell adhesion molecules. To test this possibility, we examined E-cadherin expression in the dorsolateral otocyst using confocal imaging (Fig. 2D, HH 16: n = 5; Fig. 2E, HH 18: n = 5; Fig. 2F, HH 20: n = 5; Fig. 2G, HH 24: n = 5). At HH 16, E-cadherin was broadly expressed along the entire apicobasal axis of dorsolateral otocyst cells (Fig. 2D), but with epithelial thinning and expansion during HH 18–20, E-cadherin distribution became fragmented (Figs. 2E, F). By HH 24, E-cadherin again became broadly distributed along the apicobasal axis of the now squamous dorsolateral otocyst cells (Fig. 2G). These data show that epithelial cell thinning and expansion in the dorsolateral otocyst is accompanied by changes in E-cadherin distribution, suggesting a potential role for changes in cell-cell adhesion during this localized morphogenetic event.

BMP signaling occurs in conjunction with dorsolateral otocyst thinning and expansion

BMP signaling plays a major role in patterning the dorsal otocyst. Studies in chick embryos showed that the formation of the vestibular system is sensitive to changes in BMP signaling. For example, application of Noggin, an endogenous BMP signaling inhibitor (Smith and Harland, 1992), affects the structural patterning of the cristae and causes truncation of the semicircular canals when applied during the second to third days of embryonic development (Chang et al., 1999; Gerlach et al., 2000). In addition, analysis of mouse *Bmp4* otic-conditional mutants showed that BMP4 signaling is required for the formation of the three sensory cristae and their associated non-sensory semicircular canals (Chang et al., 2008). These findings led us to ask whether BMP signaling acts earlier in development of the otocyst by regulating the rapid thinning and expansion of the dorsolateral otocyst that results in formation of the primordial canal outgrowth.

To determine whether BMP signaling occurred prior to and during dorsolateral otocyst thinning and expansion, we first asked whether BMP ligands and/or receptors were expressed in the developing chick (Suppl. Figs. 2, 3) and mouse (Suppl. Fig. 4) otocysts. We found, in agreement with previous studies (Oh et al., 1996; Wu and Oh, 1996; Daudet et al., 2007), that *Bmp4* and *7* were expressed in the chick early otocyst and adjacent mesenchyme in embryos as young as HH 16, and persisted up to HH 20, the latest stage analyzed (Suppl. Fig. 2). Moreover, BMP receptors were expressed in both the chick and mouse otocysts, with both type-I and type-II receptors being expressed (Suppl. Figs. 3, 4). Type-IA and type-II receptors were expressed within the otocyst, partially overlapping with the region of BMP activity, as assayed with pSMAD1/5/8 labeling (see below). The type-IB receptor was also detected in mouse embryos, but not in chick embryos, with a pattern similar to that of type-IA and type-II receptors.

Next, we examined in chick the expression of two genes encoding major inhibitors of BMP signaling: *Noggin* and *Smad6* (an inhibitory SMAD). *Noggin* was expressed in the mesenchyme flanking the otocyst at HH 16–20, as reported previously (Chang et al., 1999; Gerlach et al., 2000). In contrast, *cSmad6* was expressed in the ventrolateral otocyst epithelium, but not in the dorsolateral epithelial cells undergoing thinning and expansion (asterisks in Fig. 3A–D). Taken together, these results show that all components of the BMP signaling pathway are present during dorsolateral thinning and expansion of the otocyst and suggest that BMP signaling could mediate this process.

NIH-PA Author Manuscript

NIH-PA Author Manuscript

NIH-PA Author Manuscript

Finally, we examined expression of the BMP signaling indicator pSMAD1/5/8. In chick, pSMAD1/5/8 was first detected in the dorsolateral otocyst prior to the initiation of outgrowth (Fig. 3E, HH 16), and pSMAD1/5/8 staining persisted during stages of thinning and expansion (Fig. 3F, HH 18; Fig. 3G, HH 20). In mouse, a similar pattern of pSMAD1/5/8 staining was detected (Suppl. Fig. 5), but since the mouse dorsolateral otocyst is already somewhat flattened at the time of its formation, pSMAD1/5/8 staining was detected concomitantly with flattening in mouse, rather than preceding it, as in chick. These data provide strong evidence that the dorsolateral otocyst receives and responds to BMP signaling in both chick and mouse, suggesting that cell shape changes in the dorsolateral otocyst could be regulated by BMP signaling via the SMAD pathway in both organisms, and that signaling and cell behaviors underlying primordial canal outgrowth to initiate formation of the vestibular system are conserved in amniotes.

BMP signaling is sufficient to drive epithelial cell thinning and expansion in the dorsolateral otocyst

Next, we investigated whether BMP signaling is sufficient to induce changes in epithelial cell shape from columnar to squamous in the dorsolateral otocyst. *Bmp4* over expression vectors were unilaterally sonoporated into the head mesenchyme surrounding the otocyst. Over expression of *Bmp4* resulted in hyperexpansion of the dorsolateral otocyst, leading to enlargement in the diameter of the otocyst that could be readily detected in whole embryos (n = 12/40: Fig. 4A). To address the cellular mechanisms underlying enlargement of the dorsolateral otocyst, we first examined the possibility that BMP over expression increased cell proliferation. However, no differences were detected in the number of pHH3-positive cells in the dorsolateral otocyst of treated embryos as compared to control embryos (data not shown), or in the number of cells labeled with EdU after a 24-hour pulse (Suppl. Fig. 6A–C; n = 3), strongly suggesting that hyperexpansion is not the result of increased cell proliferation in the dorsolateral otocyst. Moreover, the percentage of EdU-positive cells in the dorsolateral otocyst was actually significantly decreased in embryos subjected to *Bmp4* over expression embryos as compared to that of controls, suggesting that BMP signaling inhibits cell division as it induces change in cell shape from columnar to squamous (Suppl. Fig. 6D).

Next, we asked whether over expression of *Bmp4* increased the number of pSMAD1/5/8-positive cells in the hyperexpanded area. Indeed, the hyperexpanded area of treated otocysts showed a significant increase (~30%) in the number of pSMAD1/5/8 positive cells, as compared to the dorsolateral otocyst of control embryos (n = 6/6; Fig. 4B, B’). Moreover, the width of the hyperexpanded area increased significantly (~1.5 fold) (n = 6/6; Fig. 4C, C’), and otocyst cells were flattened, with the epithelium consisting of a single nuclear layer throughout the hyperexpanded area, as assessed in sections stained with E-cadherin antibody. These results show that activation of BMP signaling is sufficient to drive dorsolateral thinning and expansion of the otocyst and provide further evidence that change in epithelial cell shape from columnar to squamous drives this morphogenetic event, resulting in the formation of the primordial canal outpouch.

BMP signaling is required for formation of the vestibular apparatus, as well as for rapid thinning and expansion of the dorsolateral otocyst

To determine whether BMP signaling is necessary for otocyst dorsolateral thinning and expansion we used unilateral sonoporation to overexpress *Noggin* and GFP in the mesenchyme surrounding the HH 13–15 otocyst and asked whether such attenuation of BMP signaling affects the formation of the primordial canal outpouch concomitant with perturbation of epithelial cell behavior in the dorsolateral otocyst. At 12 hours after sonoporation, all of the GFP-expressing cells were detected in the head mesenchyme just

NIH-PA Author Manuscript

NIH-PA Author Manuscript

NIH-PA Author Manuscript

posterior to the otocyst (Fig. 5A, A'). At HH 30 (day 10 of development), the inner ear on the Noggin-treated side of the embryo showed a dramatic alteration in the structure of the vestibular organ, including loss of all three semicircular canals and associated cristae. Despite such a dramatic alteration, the endolymphatic duct and cochlear duct developed essentially normally (n = 4/5; Fig. 5B), although the endolymphatic sac was typically truncated, and the endolymphatic duct was shorter than in controls. These results are in concert with those of others (Chang et al., 1999; Gerlach et al., 2000).

Confocal microscopic imaging of Noggin-treated otocysts at HH 24 revealed that the dorsolateral otocyst failed to form the primordial canal outpouch (n = 22/24; Fig. 5C), whereas initial ventral outgrowth (to form the cochlear duct) and dorsal outgrowth (to form the endolymphatic duct) were normal. Moreover, the dorsolateral wall of the treated otocyst failed to undergo thinning and expansion. Instead, it remained thickened, with broad and continuous apicobasal expression of E-cadherin (n = 5/5; Fig. 5D), such that at HH 18, the thickness of the dorsolateral epithelium and the distribution of E-cadherin more closely resembled that of the HH 16 control dorsolateral epithelium (cf. Figs. 5D, Noggin-treated otocyst, panels 1–4, and 2D, panels 1–4) than that of the control HH 18 control dorsolateral epithelium (cf. Figs. 5D, Noggin-treated otocysts, panels 1–4, and 2E, panels 1–4). In addition, TUNEL staining revealed no obvious differences in the number of dying cells between control and *Noggin*-treated otocysts (Suppl. Fig. 7), indicating that apoptosis is not the cause of the failure of the *Noggin*-treated dorsolateral otocyst to form the primordial canal outpouch. These data indicate that BMP signaling regulates formation of the primordial canal outpouch by regulating otocyst cell shape, which in turn drives dorsolateral otocyst thinning and expansion during the initiation of vestibular canal development.

BMP/SMAD signaling is required for dorsolateral otocyst cell flattening, resulting in formation of the primordial canal outpouch

We next asked whether BMP signaling through pSMAD1/5/8 is required for dorsolateral otocyst cell flattening and formation of the primordial canal outpouch, by treating embryos with Dorsomorphin, an inhibitor of SMAD1/5/8 phosphorylation (Yu et al., 2008). Twenty-four hours after Dorsomorphin application, treated otocysts were smaller than control otocysts (n = 7/9; Fig. 6A), with no obvious difference in the number of apoptotic cells in the dorsolateral wall of control and treated otocysts (Suppl. Fig. 8). In contrast, pSMAD1/5/8 staining was eliminated in the dorsolateral wall of treated otocysts as compared to control otocysts (Fig. 6B), indicating that phosphorylation of SMAD1/5/8 was inhibited by Dorsomorphin treatment (n = 3/3). Moreover, the expression of E-cadherin and the thickness of the dorsolateral wall in treated otocysts at HH 20 resembled those of control dorsolateral otocysts at HH 16 (cf. Fig. 6C, Dorsomorphin-treated otocysts, panels 1–4, and 2D, panels 1–4; n = 4/4), indicating that inhibition of SMAD1/5/8 phosphorylation blocks otocyst cell flattening and, consequently, thinning and expansion of dorsolateral otocyst.

Because gene expression analyses revealed that *Smad6* is predominantly expressed in epithelial cells in the ventrolateral otocyst where cells remain columnar (see Fig. 3A–D), we investigated the possibility that dorsolateral localization of otocyst thinning and expansion might be inhibited by the expression of an inhibitory SMAD such as *Smad6*. Using electroporation, a *Smad6*-expression vector was targeted to the dorsolateral epithelium of the early otocyst. Twelve hours after electroporation, gene expression was confined mainly to the dorsolateral otocyst (Fig. 7A, A'), and the extent of pSMAD1/5/8 expression was substantially reduced in the dorsolateral region (n = 4/4; Fig. 7B). Furthermore, otocysts subjected to *Smad6* over expression failed to undergo thinning and expansion of their dorsolateral wall to form the primordial canal outgrowth (n = 8/12; Fig. 7 B, C). This failure to undergo expansion was not an artifact of increasing cell apoptosis dorsolaterally in the otocyst, as no difference in TUNEL staining between control and treated otocysts could be

NIH-PA Author Manuscript

NIH-PA Author Manuscript

NIH-PA Author Manuscript

detected (Suppl. Fig. 9). Moreover, E-cadherin was broadly expressed in the dorsolateral otocyst of treated embryos at HH 20 (Fig. 7D, *Smad6*-treated embryos, panels 1–4; n = 4/4), similar to that of HH 16 normal otocysts (cf. Fig. 7D, *Smad6*-treated embryos, panels 1–4, and Fig. 2D, panels 1–4), rather than that of HH 20 control otocysts (cf. Fig. 7D, *Smad6*-treated embryos, panels 1–4, and Fig. 7D control embryo, panels 1–4, and Fig. 2D, HH 20, panels 1–4). These data suggest the hypothesis that epithelial cell flattening and formation of the primordial canal outpouch is localized to the dorsolateral otocyst by negative regulation of the BMP/SMAD pathway more ventrally, through the expression of inhibitory SMADs such as SMAD6.

DISCUSSION

BMP signaling controls at least two stages of vestibular chamber development

Gene expression and gain- and loss-of-function studies in chick, zebrafish, and mouse, show that BMP signaling from the developing sensory cristae is required for semicircular canal formation. Our results show that BMP signaling has an additional earlier function in the initial morphogenesis of the primordial canal outpouch. We found that all components of an active BMP signaling pathway—ligands, receptors, and negative and positive regulators, including pSMAD1/5/8—are present in or adjacent to the dorsolateral epithelium of the early otocyst, and that the pSMAD1/5/8-positive cells undergo a change in cell shape from columnar to squamous, resulting in rapid thinning and expansion of the dorsolateral otocyst to form the primordial canal outpouch. Furthermore, over expression of *Bmp4* results in hyperexpansion and extended mediolateral thinning of the dorsolateral otocyst, leading to the formation of an enlarged primordial canal outpouch, whereas over expression of *Noggin* or *Smad6*, or treatment with the chemical pSMAD1/5/8 inhibitor, Dorsomorphin, inhibits this process. Collectively, our studies demonstrate that BMP signaling through the SMAD1/5/8 pathway is sufficient and necessary for formation of the primordial canal outpouch, which is generated by a change in otocyst cell shape from columnar to squamous, resulting in the initiation of vestibular chamber development.

Modulation of BMP/SMAD signaling promotes formation of the primordial canal outpouch

To assess whether BMP signaling is sufficient for dorsolateral thinning and expansion, we used *Bmp4* over expression, which at early otocyst stages resulted in hyperexpansion of the dorsolateral otocyst, an increased area of SMAD signaling, and an enlarged primordial canal outpouch (Fig. 4A). This suggests that the level of BMP4 signaling determines the size of the initial otocyst outgrowth. BMP4 is a strong candidate for the endogenous regulator of the primary outgrowth of the canal pouch, as it is expressed robustly in the prospective sensory domains of the otocyst epithelium in both mouse and chick (Liu et al., 2003;Chang et al., 2008;Suppl. Fig. 2A–D). However, other *Bmps* could contribute to this regulation in vivo, as conditional deletion of *Bmp4* in the developing mouse otocyst results in a smaller, but not absent, canal pouches and, subsequently, in the failure of the semicircular canals and cristae to form (Chang et al., 2008). Moreover, we show that in chick, *Bmp7* is also expressed at the right time and place to potentially play a role.

In addition to quantitative and qualitative regulation of ligand expression, endogenous inhibitors of BMP signaling are likely to be involved in the quantitative control of BMP signaling during the initial canal pouch outgrowth. Noggin binds with strong affinity to BMP4 in the extracellular space (Zimmerman et al., 1996). During thinning and expansion of the dorsolateral otocyst, Noggin is expressed in close association with the *Bmp4* domain (Chang et al., 1999; Gerlach et al., 2000; Bok et al., 2007b). Thus, Noggin is in a position to regulate the precise size and location within the otocyst of the primordial canal outpouch. Our study shows that Noggin over expression in the head mesenchyme surrounding the early

NIH-PA Author Manuscript

NIH-PA Author Manuscript

NIH-PA Author Manuscript

otocyst prevents formation of the primordial canal outpouch and, subsequently, leads to a complete loss of the three semicircular canals and cristae (Fig. 5). Intriguingly, knock out of Noggin in mouse embryos results in the opposite effect, causing an anteriorly enlarged canal pouch, with an extended anterior semicircular canal forming during subsequent development (Bok et al., 2007b). Thus, Noggin likely acts as an endogenous negative regulator of BMP signaling during formation of the primordial canal outpouch.

Although BMP signaling can occur through both SMAD-dependent and SMAD-independent pathways (Sugimori et al., 2005; Beck and Carethers, 2007), the result that *Smad6* over expression (as well as Dorsomorphin treatment) blocks dorsolateral thinning and expansion and primordial canal outpouching indicates that at least the SMAD-dependent pathway is required for formation of the primordial canal outpouch. SMAD6 is an intracellular inhibitor of BMP/SMAD signaling, which acts by binding to the type-I receptor, thus preventing phosphorylation of SMAD1/5/8 or competing with SMAD4 for heteromeric complex formation (Itóh et al., 2000; Massagué, 2000; Moustakas et al., 2001). *Smad6*-defective mice form bony structures within their aortic wall, a process reminiscent of endochondral bone formation, which is mediated by BMP signaling (Galvin et al., 2000). During formation of the otic capsule, SMAD6/7 negatively regulates BMP/SMAD-regulated chondogenesis (Liu et al., 2007). Our results show that *Smad6* is expressed within the lateral otocyst epithelium adjacent to the *Bmp* expression domain, but it is not expressed within the dorsolateral otocyst where thinning and expansion occurs (Fig. 3A–D). Over expression of *Smad6* within the dorsolateral otocyst reduced pSMAD1/5/8 staining in the dorsolateral otocyst and prevented thinning and expansion of the otocyst, indicating that SMAD6 can act as an intracellular negative regulator of BMP/SMAD signaling during formation of the primordial canal outpouch.

BMP/SMAD signaling controls epithelial cell flattening and E-cadherin fragmentation, resulting in formation of the primordial canal outpouch

Epithelial morphogenesis is a crucial event in the formation of both organ rudiments and definitive organs in multicellular organisms. Epithelia can be classified into several types based on the shape of their cells, including columnar epithelia, which contain elongated (columnar) cells having extended basolateral domains; cuboidal epithelia, which contain cuboidal cells that are equally tall as they are wide; and squamous epithelia, which contain flattened (squamous) cells with extended apical domains. Epithelia are not static, but can change their shape, especially during development, and in some disease states, such as metastasis.

The wall of the early chick otocyst initially consists of a pseudostratified columnar epithelium containing multiple nuclear layers. We showed that over time, the dorsolateral otocyst epithelium becomes cuboidal and subsequently squamous, resulting in rapid and localized thinning and expansion of the otocyst wall and formation of the primordial canal outpouch. Similar changes in cell shapes are common in a variety of developing epithelia. For example, branching morphogenesis during lung development is accompanied by changes in epithelial cell shape along the proximal-distal axis of the lung bud. In early stages of budding, the bud wall consists of tall columnar epithelium. Later, the distal epithelium transforms into low cuboidal or squamous, whereas the proximal epithelium remains columnar (Burri, 1984; Weaver et al., 1999). Moreover, during mammary gland formation, the milk line is initially defined by a slight thickening and stratification of epithelium. Later, this epithelium becomes columnar and forms a series of placodes (Hens and Wysolmerski, 2005; Robinson, 2007). In addition, during tumorigenesis, squamous cell carcinoma is believed to derive from columnar epithelia that undergo transformation (Saffiotti et al., 1967; Iwasa et al., 2007).

NIH-PA Author Manuscript

NIH-PA Author Manuscript

NIH-PA Author Manuscript

BMP signaling is implicated in the examples of epithelial morphogenesis just described. In transgenic mice in which Noggin expression is driven to the distal respiratory epithelium using the *Surfactant Protein-C* (Sp-C) promoter, normal changes in cell shape from columnar to low cuboidal are inhibited (Weaver et al., 1999). Additionally, in Sp-C-dnAlk6 transgenic mice, the cells in the distal epithelium of the lungs are taller than those in the epithelium of wild type lungs (Weaver et al., 1999). During mammary gland formation, BMP signaling promotes thickening of the ectoderm to form the mammary placodes (Cho et al., 2006). Furthermore, BMP6 is upregulated in esophageal squamous cell carcinoma (Raida et al., 1999; Stoner and Gupta, 2001). Our present results are consistent with these reports in that we show that BMP signaling is sufficient and necessary for columnar to squamous cell shape changes in the dorsolateral otocyst. Over expression of *Bmp4* resulted in enhanced epithelial cell flattening in the dorsolateral otocyst, and this change was arrested by attenuation of BMP signaling using *Noggin*, Dorsomorphin, or *Smad6* treatment.

Recent studies showed that adherens junction (AJ) E-cadherin is necessary for epithelial cell flattening. Epiboly, an early morphogenetic event occurring during gastrulation in a variety of vertebrate embryos including teleost embryos, involves spreading and flattening of the blastoderm over the yolk. However, in *half-backed* (*hab*) mutants—which harbor a mutation in the teleost ortholog of E-cadherin—epiblast cells fail to undergo flattening, and epiboly is arrested (Kane et al., 2005). Follicle cells in *D. melanogaster* initially have a cuboidal shape and form a monolayer around the germline cyst. During subsequent development, they progressively differentiate into a population of squamous or columnar cells. As this cell shape change occurs, E-cadherin distribution is dynamically altered. Initially, E-cadherin is expressed in a pattern that outlines the hexagonal shape of follicular cells, indicating that AJs are present along the apical circumferences of follicle cells, but as cells flatten, E-caherin expression becomes fragmented (Grammont, 2007). We noted similar dynamic expression patterns of E-cadherin during change in cell shape from columnar to squamous in the dorsolateral otocyst, supporting the possibility that alteration of E-cadherin distribution plays a key role in regulating of epithelial cell flattening.

Although the exact relationship between BMP signaling and alteration of E-cadherin distribution is unknown, one possibility is that epithelial cell flattening in the dorsolateral otocyst involves recycling of E-cadherin via endocytosis. Endocytosis of E-cadherin has been observed during various cellular contexts such as during mitosis, cell scattering, and epithelial-mesenchymal transition (EMT) (Bauer et al., 1998; Kamei et al., 1999; Le et al., 1999; Janda et al., 2006). The molecular mechanism underlying induction of E-cadherin endocytosis involves the activation of tyrosine kinases such as Src (c-Src). Activated Src physically binds to and enhances tyrosine phosphorylation of E-cadherin and its binding proteins, leading to the recruitment of an E3 ubiquitin ligase that ubiquitinates and induces internalization of the E-cadherin complex. The complex is then sorted into lysosomes for protein degradation. Activation of Src has been considered as one of the key events inducing E-cadherin endocytosis. Future studies will determine whether E-cadherin endocytosis is directly involved in otocyst cell flattening and whether BMP signaling induces E-cadherin endocytosis via Src activation during formation of the primordial canal outgrowth.

Supplementary Material

Refer to Web version on PubMed Central for supplementary material.

Acknowledgments

We thank our colleagues for providing probes (see Materials and Methods). Samantha Gliford and Steven Bleyl provided the mouse ear reconstructions, and Lisa Urness collected and provided mouse embryos, as well as in situ

NIH-PA Author Manuscript

NIH-PA Author Manuscript

NIH-PA Author Manuscript

hybridization probes for type-I and –II BMP receptors. Finally, we acknowledge essential financial support from grant no. DC004185 from the NIH.

REFERENCES

Affolter M, Zeller R, Caussinus E. Tissue remodelling through branching morphogenesis. Nat Rev Mol Cell Biol. 2009; 10:831–842. [PubMed: 19888266]

Andrew DJ, Ewald AJ. Morphogenesis of epithelial tubes: Insights into tube formation, elongation, and elaboration. Dev Biol. 2010; 341:34–55. [PubMed: 19778532]

Antonelli PJ, Varela AE, Mancuso AA. Diagnostic yield of high-resolution computed tomography for pediatric sensorineural hearing loss. Laryngoscope. 1999; 109:1642–1647. [PubMed: 10522936]

Barald KF, Kelley MW. From placode to polarization: new tunes in inner ear development. Development. 2004; 131:4119–4130. [PubMed: 15319325]

Bauer A, Lickert H, Kemler R, Stappert J. Modification of the E-cadherin-catenin complex in mitotic Madin-Darby canine kidney epithelial cells. J Biol Chem. 1998; 273:28314–28321. [PubMed: 9774455]

Beck SE, Carethers JM. BMP suppresses PTEN expression via RAS/ERK signaling. Cancer Biol Ther. 2007; 6:1313–1317. [PubMed: 18059158]

Bissonnette JP, Fekete DM. Standard atlas of the gross anatomy of the developing inner ear of the chicken. J Comp Neurol. 1996; 368:620–630. [PubMed: 8744448]

Bok J, Chang W, Wu DK. Patterning and morphogenesis of the vertebrate inner ear. Int J Dev Biol. 2007a; 51:521–533. [PubMed: 17891714]

Bok J, Brunet LJ, Howard O, Burton Q, Wu DK. Role of hindbrain in inner ear morphogenesis: analysis of Noggin knockout mice. Dev Biol. 2007b; 311:69–78. [PubMed: 17900554]

Bok J, Dolson DK, Hill P, Rüther U, Epstein DJ, Wu DK. Opposing gradients of Gli repressor and activators mediate Shh signaling along the dorsoventral axis of the inner ear. Development. 2007c; 134:1713–1722. [PubMed: 17395647]

Burri PH. Fetal and postnatal development of the lung. Annu Rev Physiol. 1984; 46:617–628. [PubMed: 6370120]

Carthew RW. Adhesion proteins and the control of cell shape. Curr Opin Genet Dev. 2005; 15:358–363. [PubMed: 15963712]

Chang W, Nunes FD, De Jesus-Escobar JM, Harland R, Wu DK. Ectopic noggin blocks sensory and nonsensory organ morphogenesis in the chicken inner ear. Dev Biol. 1999; 216:369–381. [PubMed: 10588886]

Chang W, ten Dijke P, Wu DK. BMP pathways are involved in otic capsule formation and epithelial-mesenchymal signaling in the developing chicken inner ear. Dev Biol. 2002; 251:380–394. [PubMed: 12435365]

Chang, W.; Cole, L.; Cantos, R.; Wu, D. Molecular genetics of vestibular organ development. In: Highstein, SM.; Fay, RR.; Popper, AN., editors. Springer Handbook of Auditory Research. Vol. Vol. 19. 2004a. p. 1-46.The Vestibular System

Chang W, Brigande JV, Fekete DM, Wu DK. The development of semicircular canals in the inner ear: role of FGFs in sensory cristae. Development. 2004b; 131:4201–4211. [PubMed: 15280215]

Chang W, Lin Z, Kulessa H, Hebert J, Hogan BLM, Wu DK. Bmp4 is essential for the formation of the vestibular apparatus that detects angular head movements. PLoS Genet. 2008; 4:e1000050. [PubMed: 18404215]

Cho K-W, Kim J-Y, Song S-J, Farrell E, Eblaghie MC, Kim H-J, Tickle C, Jung H-S. Molecular interactions between Tbx3 and Bmp4 and a model for dorsoventral positioning of mammary gland development. Proc Natl Acad Sci USA. 2006; 103:16788–16793. [PubMed: 17071745]

Dabdoub A, Donohue MJ, Brennan A, Wolf V, Montcouquiol M, Sassoon DA, Hseih J-C, Rubin JS, Salinas PC, Kelley MW. Wnt signaling mediates reorientation of outer hair cell stereociliary bundles in the mammalian cochlea. Development. 2003; 130:2375–2384. [PubMed: 12702652]

Dabdoub A, Kelley MW. Planar cell polarity and a potential role for a Wnt morphogen gradient in stereociliary bundle orientation in the mammalian inner ear. J Neurobiol. 2005; 64:446–457. [PubMed: 16041762]

NIH-PA Author Manuscript

NIH-PA Author Manuscript

NIH-PA Author Manuscript

Daudet N, Ariza-McNaughton L, Lewis J. Notch signalling is needed to maintain, but not to initiate, the formation of prosensory patches in the chick inner ear. Development. 2007; 134:2369–2378. [PubMed: 17537801]

Fekete DM, Homburger SA, Waring MT, Riedl AE, Garcia LF. Involvement of programmed cell death in morphogenesis of the vertebrate inner ear. Development. 1997; 124:2451–2461. [PubMed: 9199371]

Galvin KM, Donovan MJ, Lynch CA, Meyer RI, Paul RJ, Lorenz JN, Fairchild-Huntress V, Dixon KL, Dunmore JH, Gimbrone MA, Falb D, Huszar D. A role for smad6 in development and homeostasis of the cardiovascular system. Nat Genet. 2000; 24:171–174. [PubMed: 10655064]

Gerlach LM, Hutson MR, Germiller JA, Nguyen-Luu D, Victor JC, Barald KF. Addition of the BMP4 antagonist, noggin, disrupts avian inner ear development. Development. 2000; 127:45–54. [PubMed: 10654599]

Grammont M. Adherens junction remodeling by the Notch pathway in Drosophila melanogaster oogenesis. J Cell Biol. 2007; 177:139–150. [PubMed: 17420294]

Grimmer JF, Hedlund G. Vestibular symptoms in children with enlarged vestibular aqueduct anomaly. International Journal of Pediatric Otorhinolaryngology. 2007; 71:275–282. [PubMed: 17113162]

Haddon CM, Lewis JH. Hyaluronan as a propellant for epithelial movement: the development of semicircular canals in the inner ear of Xenopus. Development. 1991; 112:541–550. [PubMed: 1794322]

Hamburger V, Hamilton HL. A series of normal stages in the development of the chick embryo. Dev Dyn. 1992; 195:231–272. (reprinted from Hamburger, V., Hamilton, H. L., 1951. A series of normal stages in the development of the chick embryo. J Morph., 88, 49–92). [PubMed: 1304821]

Hammond KL, Loynes HE, Mowbray C, Runke G, Hammerschmidt M, Mullins MC, Hildreth V, Chaudhry B, Whitfield TT. A late role for bmp2b in the morphogenesis of semicircular canal ducts in the zebrafish inner ear. PLoS ONE. 2009; 4:e4368. [PubMed: 19190757]

Hammond KL, Van Eeden FJM, Whitfield TT. Repression of Hedgehog signalling is required for the acquisition of dorsolateral cell fates in the zebrafish otic vesicle. Development. 2010; 137:1361–1371. [PubMed: 20223756]

Hatch EP, Noyes CA, Wang X, Wright TJ, Mansour SL. Fgf3 is required for dorsal patterning and morphogenesis of the inner ear epithelium. Development. 2007; 134:3615–3625. [PubMed: 17855431]

Hens JR, Wysolmerski JJ. Key stages of mammary gland development: molecular mechanisms involved in the formation of the embryonic mammary gland. Breast Cancer Res. 2005; 7:220–224. [PubMed: 16168142]

Hwang CH, Guo D, Harris MA, Howard O, Mishina Y, Gan L, Harris SE, Wu DK. Role of bone morphogenetic proteins on cochlear hair cell formation: analyses of Noggin and Bmp2 mutant mice. Dev Dyn. 2010; 239:505–513. [PubMed: 20063299]

Itóh S, Itoh F, Goumans MJ, Ten Dijke P. Signaling of transforming growth factor-beta family members through Smad proteins. Eur J Biochem. 2000; 267:6954–6967. [PubMed: 11106403]

Iwasa A, Oda Y, Kaneki E, Ohishi Y, Kurihara S, Yamada T, Hirakawa T, Wake N, Tsuneyoshi M. Squamous cell carcinoma arising in mature cystic teratoma of the ovary: an immunohistochemical analysis of its tumorigenesis. Histopathology. 2007; 51:98–104. [PubMed: 17542994]

Janda E, Nevolo M, Lehmann K, Downward J, Beug H, Grieco M. Raf plus TGFbeta-dependent EMT is initiated by endocytosis and lysosomal degradation of E-cadherin. Oncogene. 2006; 25:7117–7130. [PubMed: 16751808]

Kamei T, Matozaki T, Sakisaka T, Kodama A, Yokoyama S, Peng YF, Nakano K, Takaishi K, Takai Y. Coendocytosis of cadherin and c-Met coupled to disruption of cell-cell adhesion in MDCK cells--regulation by Rho, Rac and Rab small G proteins. Oncogene. 1999; 18:6776–6784. [PubMed: 10597286]

Kane DA, McFarland KN, Warga RM. Mutations in half baked/E-cadherin block cell behaviors that are necessary for teleost epiboly. Development. 2005; 132:1105–1116. [PubMed: 15689372]

Kelly M, Chen P. Shaping the mammalian auditory sensory organ by the planar cell polarity pathway. Int J Dev Biol. 2007; 51:535–547. [PubMed: 17891715]

NIH-PA Author Manuscript

NIH-PA Author Manuscript

NIH-PA Author Manuscript

Koo SK, Hill JK, Hwang CH, Lin ZS, Millen KJ, Wu DK. Lmx1a maintains proper neurogenic, sensory, and non-sensory domains in the mammalian inner ear. Dev Biol. 2009; 333:14–25. [PubMed: 19540218]

Ladher RK, O'Neill P, Begbie J. From shared lineage to estranged function: the development of the inner ear and epibranchial placodes. Development. 2010; 137:1–9.

Lang H, Bever MM, Fekete DM. Cell proliferation and cell death in the developing chick inner ear: spatial and temporal patterns. J Comp Neurol. 2000; 417:205–220. [PubMed: 10660898]

Le TL, Yap AS, Stow JL. Recycling of E-cadherin: a potential mechanism for regulating cadherin dynamics. J Cell Biol. 1999; 146:219–232. [PubMed: 10402472]

Léger S, Brand M. Fgf8 and Fgf3 are required for zebrafish ear placode induction, maintenance and inner ear patterning. Mech Dev. 2002; 119:91–108. [PubMed: 12385757]

Liu W, Oh SH, Kang Yk Yk, Li G, Doan TM, Little M, Li L, Ahn K, Crenshaw EB, Frenz DA. Bone morphogenetic protein 4 (BMP4): a regulator of capsule chondrogenesis in the developing mouse inner ear. Dev Dyn. 2003; 226:427–438. [PubMed: 12619129]

Liu W, Butts S, Kim H, Frenz DA. Negative regulation of otic capsule chondrogenesis: it can make you Smad. Ann N Y Acad Sci. 2007; 1116:141–148. [PubMed: 17584986]

Manoussaki D, Chadwick RS, Ketten DR, Arruda J, Dimitriadis EK, O'Malley JT. The influence of cochlear shape on low-frequency hearing. Proc Natl Acad Sci USA. 2008; 105:6162–6166. [PubMed: 18413615]

Mansour SL, Schoenwolf GC. Morphogenesis of the inner ear. Auditory handbook. 2005:1–42.

Mansour SL, Goddard JM, Capecchi MR. Mice homozygous for a targeted disruption of the proto-oncogene int-2 have developmental defects in the tail and inner ear. Development. 1993; 117:13–28. [PubMed: 8223243]

Martin P, Swanson GJ. Descriptive and experimental analysis of the epithelial remodellings that control semicircular canal formation in the developing mouse inner ear. Dev Biol. 1993; 159:549–558. [PubMed: 8405678]

Massagué J. How cells read TGF-beta signals. Nat Rev Mol Cell Biol. 2000; 1:169–178. [PubMed: 11252892]

Montcouquiol M, Kelley MW. Planar and vertical signals control cellular differentiation and patterning in the mammalian cochlea. J Neurosci. 2003; 23:9469–9478. [PubMed: 14561877]

Montcouquiol M, Rachel RA, Lanford PJ, Copeland NG, Jenkins NA, Kelley MW. Identification of Vangl2 and Scrb1 as planar polarity genes in mammals. Nature. 2003; 423:173–177. [PubMed: 12724779]

Montcouquiol M, Sans N, Huss D, Kach J, Dickman JD, Forge A, Rachel RA, Copeland NG, Jenkins NA, Bogani D, Murdoch J, Warchol ME, Wenthold RJ, Kelley MW. Asymmetric localization of Vangl2 and Fz3 indicate novel mechanisms for planar cell polarity in mammals. J Neurosci. 2006; 26:5265–5275. [PubMed: 16687519]

Morsli H, Choo D, Ryan A, Johnson R, Wu DK. Development of the mouse inner ear and origin of its sensory organs. J Neurosci. 1998; 18:3327–3335. [PubMed: 9547240]

Moustakas A, Souchelnytskyi S, Heldin CH. Smad regulation in TGF-beta signal transduction. J Cell Sci. 2001; 114:4359–4369. [PubMed: 11792802]

Nichols DH, Pauley S, Jahan I, Beisel KW, Millen KJ, Fritzsch B. Lmx1a is required for segregation of sensory epithelia and normal ear histogenesis and morphogenesis. Cell Tissue Res. 2008; 334:339–358. [PubMed: 18985389]

Oh SH, Johnson R, Wu DK. Differential expression of bone morphogenetic proteins in the developing vestibular and auditory sensory organs. J Neurosci. 1996; 16:6463–6475. [PubMed: 8815925]

Ohuchi H, Yasue A, Ono K, Sasaoka S, Tomonari S, Takagi A, Itakura M, Moriyama K, Noji S, Nohno T. Identification of cis-element regulating expression of the mouse Fgf10 gene during inner ear development. Dev Dyn. 2005; 233:177–187. [PubMed: 15765517]

Ohyama T, Groves AK, Martin K. The first steps towards hearing: mechanisms of otic placode induction. Int J Dev Biol. 2007; 51:463–472. [PubMed: 17891709]

Pauley S, Wright TJ, Pirvola U, Ornitz D, Beisel K, Fritzsch B. Expression and function of FGF10 in mammalian inner ear development. Dev Dyn. 2003; 227:203–215. [PubMed: 12761848]

NIH-PA Author Manuscript

NIH-PA Author Manuscript

NIH-PA Author Manuscript

Purcell D, Johnson J, Fischbein N, Lalwani AK. Establishment of normative cochlear and vestibular measurements to aid in the diagnosis of inner ear malformations. Otolaryngol Head Neck Surg. 2003; 128:78–87. [PubMed: 12574763]

Qian D, Jones C, Rzadzinska A, Mark S, Zhang X, Steel KP, Dai X, Chen P. Wnt5a functions in planar cell polarity regulation in mice. Dev Biol. 2007; 306:121–133. [PubMed: 17433286]

Raida M, Sarbia M, Clement JH, Adam S, Gabbert HE, Höffken K. Expression, regulation and clinical significance of bone morphogenetic protein 6 in esophageal squamous-cell carcinoma. Int J Cancer. 1999; 83:38–44. [PubMed: 10449605]

Riccomagno MM, Martinu L, Mulheisen M, Wu DK, Epstein DJ. Specification of the mammalian cochlea is dependent on Sonic hedgehog. Genes Dev. 2002; 16:2365–2378. [PubMed: 12231626]

Riccomagno MM, Takada S, Epstein DJ. Wnt-dependent regulation of inner ear morphogenesis is balanced by the opposing and supporting roles of Shh. Genes Dev. 2005; 19:1612–1623. [PubMed: 15961523]

Rida P, Chen P. Line up and listen: Planar cell polarity regulation in the mammalian inner ear. Semin Cell Dev Biol. 2009

Robinson GW. Cooperation of signalling pathways in embryonic mammary gland development. Nat Rev Genet. 2007; 8:963–972. [PubMed: 18007652]

Saffiotti U, Montesano R, Sellakumar AR, Borg SA. Experimental cancer of the lung. Inhibition by vitamin A of the induction of tracheobronchial squamous metaplasia and squamous cell tumors. Cancer. 1967; 20:857–864. [PubMed: 6024294]

Sapède D, Pujades C. Hedgehog signaling governs the development of otic sensory epithelium and its associated innervation in zebrafish. J Neurosci. 2010; 30:3612–3623. [PubMed: 20219995]

Smith CW, Harland MR. Expression Cloning of noggin, a New Dorsalizing Factor Localized to the Spemann Organizer in Xenopus Embryos. Cell. 1992; 70:829–840. [PubMed: 1339313]

Stoner GD, Gupta A. Etiology and chemoprevention of esophageal squamous cell carcinoma. Carcinogenesis. 2001; 22:1737–1746. [PubMed: 11698334]

Sugimori K, Matsui K, Motomura H, Tokoro T, Wang J, Higa S, Kimura T, Kitajima I. BMP-2 prevents apoptosis of the N1511 chondrocytic cell line through PI3K/Akt-mediated NF-kappaB activation. J Bone Miner Metab. 2005; 23:411–419. [PubMed: 16261446]

Wang J, Mark S, Zhang X, Qian D, Yoo S-J, Radde-Gallwitz K, Zhang Y, Lin X, Collazo A, Wynshaw-Boris A, Chen P. Regulation of polarized extension and planar cell polarity in the cochlea by the vertebrate PCP pathway. Nat Genet. 2005; 37:980–985. [PubMed: 16116426]

Warren M, Puskarczyk K, Chapman SC. Chick embryo proliferation studies using EdU labeling. Dev Dyn. 2009; 238:944–949. [PubMed: 19253396]

Weaver M, Yingling JM, Dunn NR, Bellusci S, Hogan BL. Bmp signaling regulates proximal-distal differentiation of endoderm in mouse lung development. Development. 1999; 126:4005–4015. [PubMed: 10457010]

Whitfield TT, Hammond KL. Axial patterning in the developing vertebrate inner ear. Int J Dev Biol. 2007; 51:507–520. [PubMed: 17891713]

Worden BF, Blevins NH. Pediatric vestibulopathy and pseudovestibulopathy: differential diagnosis and management. Current opinion in otolaryngology & head and neck surgery. 2007; 15:304–309. [PubMed: 17823544]

Wu C-C, Chen Y-S, Chen P-J, Hsu C-J. Common clinical features of children with enlarged vestibular aqueduct and Mondini dysplasia. Laryngoscope. 2005; 115:132–137. [PubMed: 15630381]

Wu DK, Oh SH. Sensory organ generation in the chick inner ear. J Neurosci. 1996; 16:6454–6462. [PubMed: 8815924]

Yamamoto N, Okano T, Ma X, Adelstein RS, Kelley MW. Myosin II regulates extension, growth and patterning in the mammalian cochlear duct. Development. 2009; 136:1977–1986. [PubMed: 19439495]

Yu PB, Hong CC, Sachidanandan C, Babitt JL, Deng DY, Hoyng SA, Lin HY, Bloch KD, Peterson RT. Dorsomorphin inhibits BMP signals required for embryogenesis and iron metabolism. Nat Chem Biol. 2008; 18:33–41. [PubMed: 18026094]

NIH-PA Author Manuscript

NIH-PA Author Manuscript

NIH-PA Author Manuscript

Zelarayan LC, Vendrell V, Alvarez Y, Domínguez-Frutos E, Theil T, Alonso MT, Maconochie M, Schimmang T. Differential requirements for FGF3, FGF8 and FGF10 during inner ear development. Dev Biol. 2007; 308:379–391. [PubMed: 17601531]

Zimmerman LB, De Jesús-Escobar JM, Harland RM. The Spemann organizer signal noggin binds and inactivates bone morphogenetic protein 4. Cell. 1996; 86:599–606. [PubMed: 8752214]

NIH-PA Author Manuscript
NIH-PA Author Manuscript
NIH-PA Author Manuscript

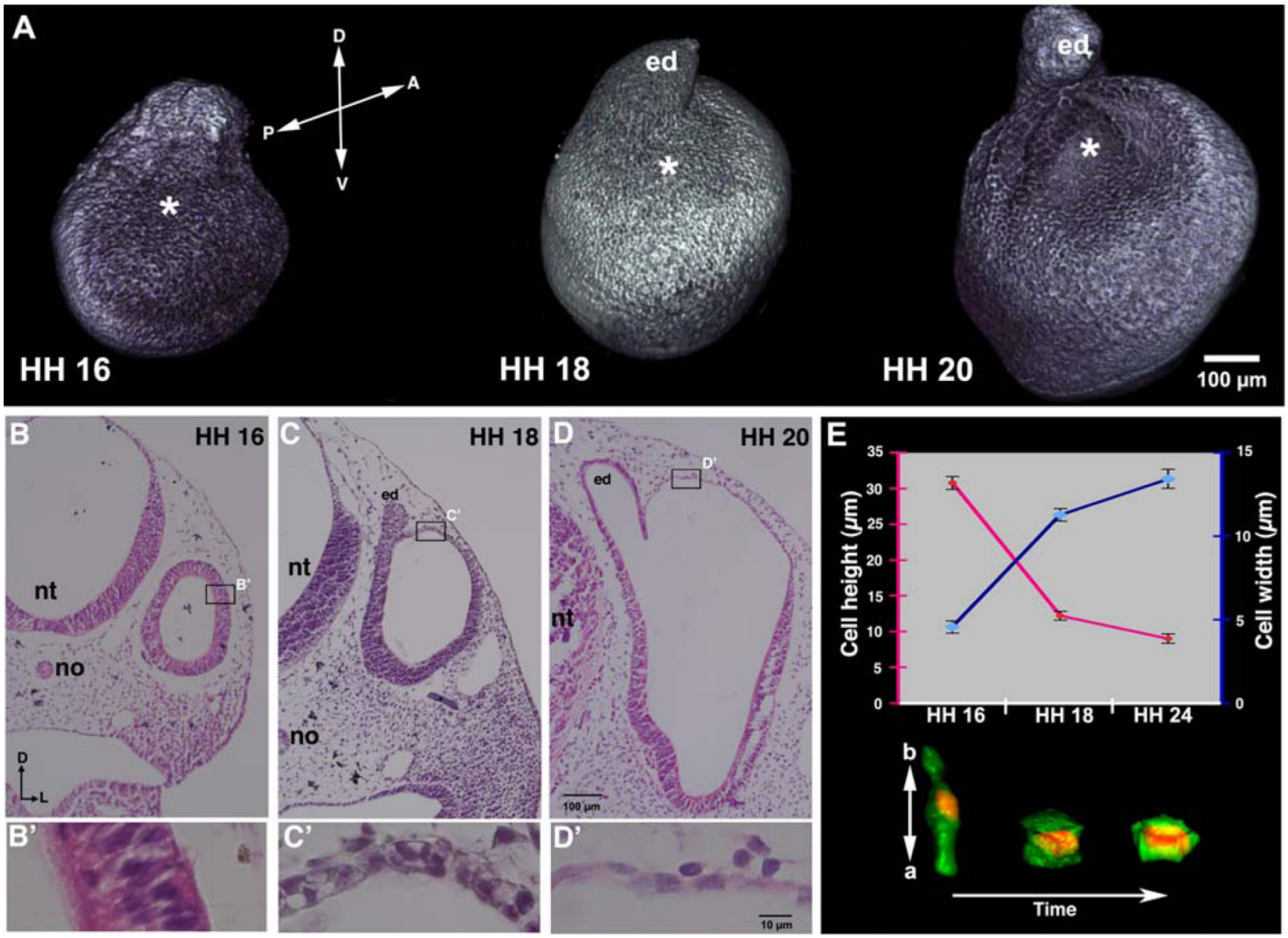

Figure 1. During inner ear development the dorsolateral wall of the chick otocyst undergoes rapid thinning and expansion, driven by cell-shape change, heralding the onset of region-specific morphogenesis of the otocyst

(A) Confocal reconstructions of anti-E-cadherin-labeled otocysts at HH 16, 18, and 20. Asterisks mark the dorsolateral wall of the otocyst that undergoes rapid thinning and expansion. D, dorsal; V, ventral; A, anterior; P, posterior; ed, endolymphatic duct. (B–D) Transverse H&E-stained sections of otocysts at HH 16–20. (B'-D') Enlargements of the boxes in B–D showing epithelial thinning in the dorsolateral otocyst wall during its expansion. D, dorsal; L, lateral; nt, neural tube; no, notochord; ed, endolymphatic duct. (E) Graph showing measurements of cells (maximal mean cell heights, red line, measured in the apicobasal dimension of the epithelium; maximal mean cell widths, blue line, measured at the widest part of the cell, which coincided with the mid apicobasal level of the nucleus; bars indicate standard error of the mean) and confocal reconstruction of cell shapes (red, Hoechst staining of nuclei; green, cytoplasmic GFP transfected into the dorsolateral otocyst at HH 15) over about 2.5 days of development showing that the pseudostratified columnar epithelial cells of the dorsolateral otocyst at HH 16 transform into cuboidal epithelial cells by HH 18, and then into squamous epithelial cells by HH 20 (HH 24 is pictured and measured). a, apical side of cell; b, basal side of cell.

NIH-PA Author Manuscript
NIH-PA Author Manuscript
NIH-PA Author Manuscript

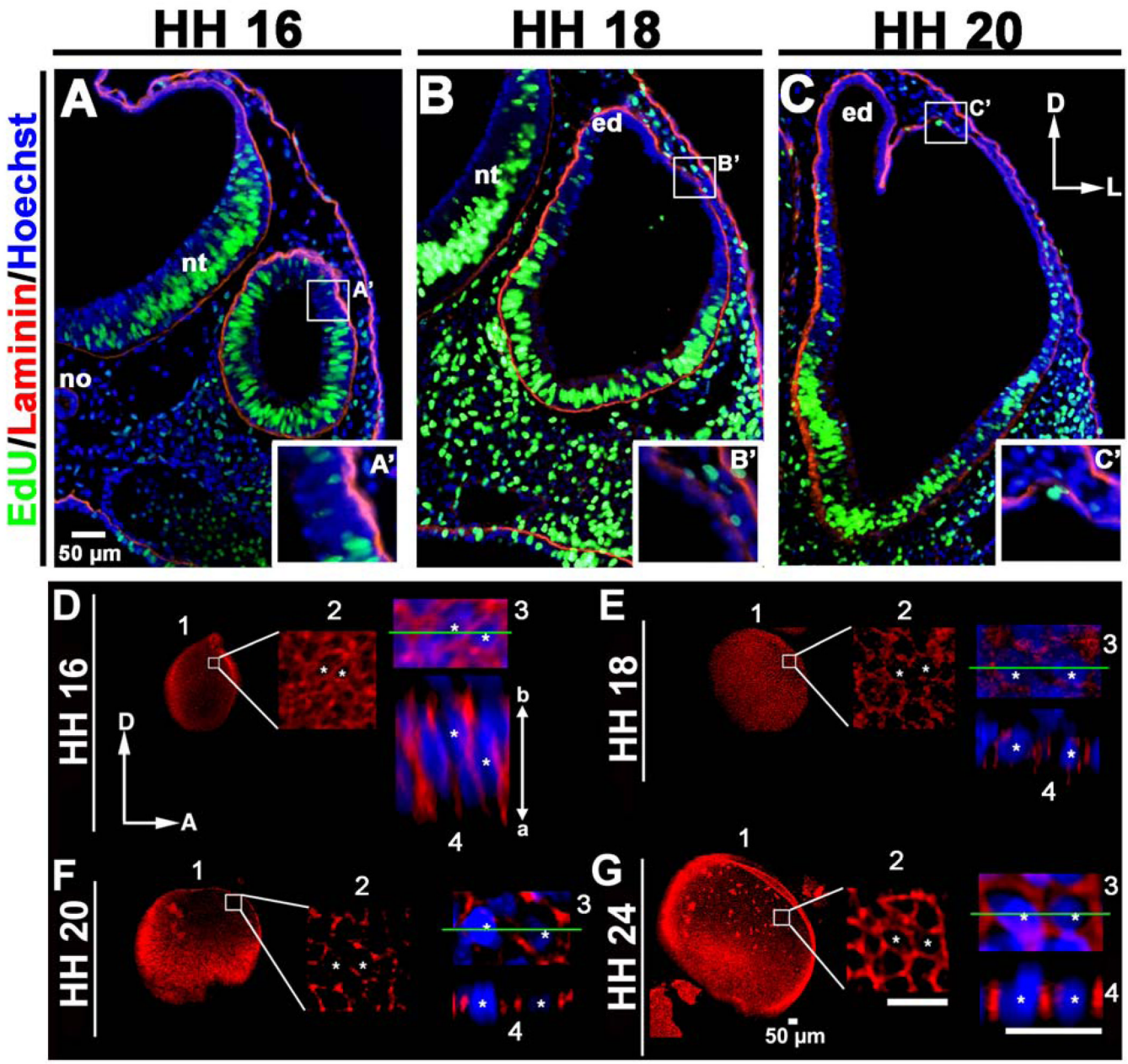

Figure 2. Increased cell proliferation does not drive expansion of the chick dorsolateral otocyst

(A–C) Transverse sections of embryos pulsed for 2 hours with EdU (green), counterstained with anti-laminin (red) and Hoechst stain (blue) showing that the region that will undergo dorsolateral expansion (boxed, HH 16), or was undergoing dorsolateral expansion at the time the embryo was collected (boxed, HH 18 and 20). The dorsolateral otocyst contains few EdU-positive (i.e., mitotic cells in the S-phase of the cell cycle) cells, as compared to other regions of the developing otocyst, indicating that cell proliferation is not increased in the dorsolateral otocyst during its rapid expansion. D, dorsal; L, lateral; no, notochord; nt, neural tube; ed, endolymphatic duct. (A'-C') Enlargements of the boxes in A–C showing epithelial thinning in the dorsolateral otocyst during its expansion. (D–G) Confocal imaging showing that E-cadherin (red; cell nuclei labeled with Hoechst staining, blue) is broadly distributed along the entire apicobasal (a–b) axis of the dorsolateral epithelium at HH 16,

and then fragments as dorsolateral epithelial cells undergo thinning during HH 18–24. 1, panel showing the entire otocyst. 2, boxed area in panel 1 enlarged. 3, area in panel 2 containing two cells marked with asterisks enlarged. 4, panel showing a lateral view of the epithelium at the level of the green line in panel 3. D, dorsal; A, anterior.

NIH-PA Author Manuscript
NIH-PA Author Manuscript
NIH-PA Author Manuscript

NIH-PA Author Manuscript
NIH-PA Author Manuscript
NIH-PA Author Manuscript

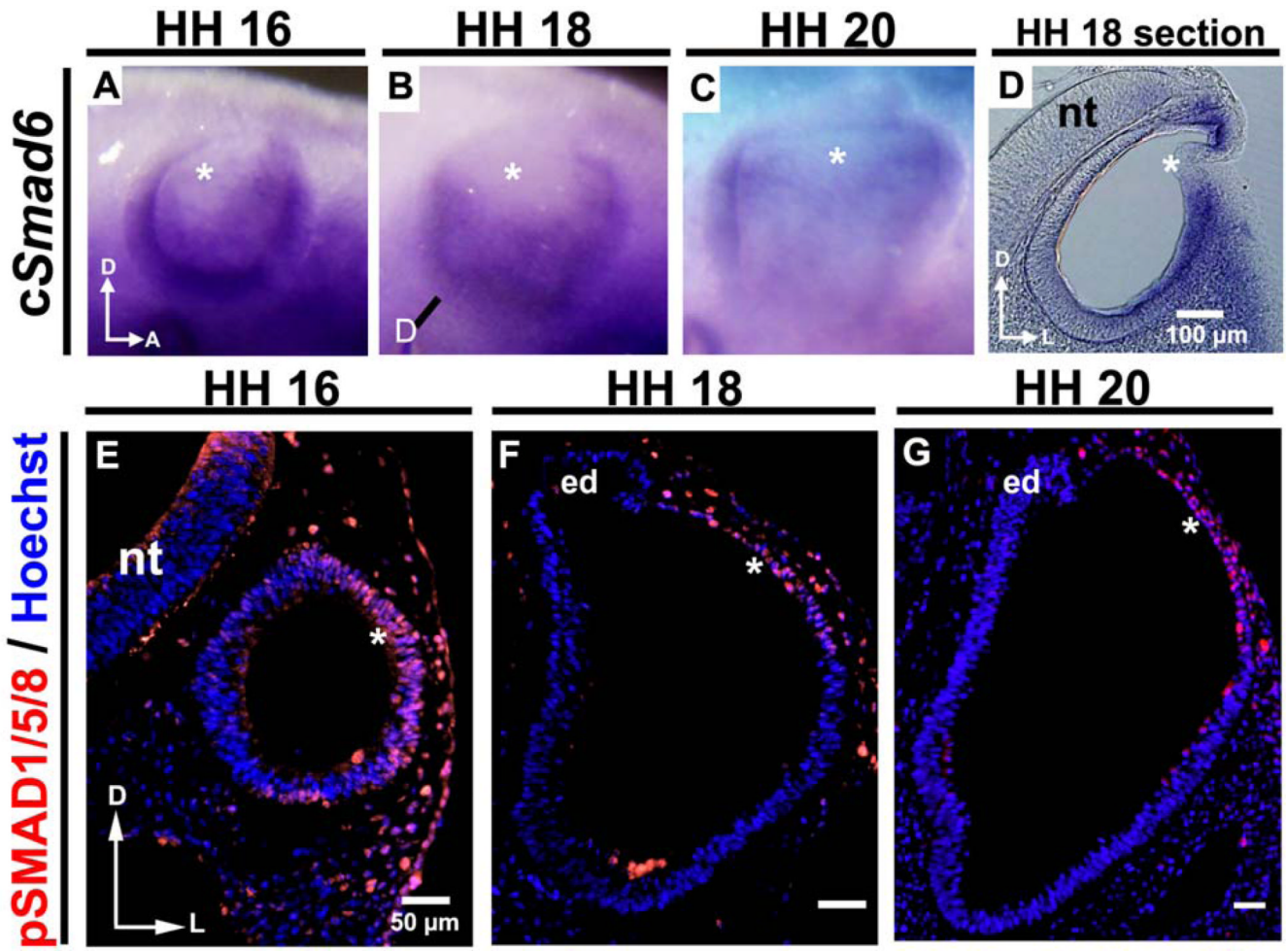

Figure 3. *Smad6*, an inhibitor of BMP signaling, is expressed only in the chick ventrolateral otocyst during its thinning and expansion, whereas pSMAD1/5/8 is expressed in the dorsolateral otocyst, indicating that this portion of the otocyst receives and responds to BMP signaling

(A–C) As shown by whole mount in situ hybridization, *Smad6*, an inhibitor of BMP signaling, is expressed in the otocyst (but not in its dorsolateral wall; asterisks) during HH 16–20 when rapid thinning and expansion occurs (HH 16: n = 6; HH 18: n = 18; HH 20: n = 16). The line in (B) marks the level of the section shown in (D). Sections (D) reveal more clearly that expression occurs only in the ventrolateral wall of the otocyst, not in its dorsolateral wall (asterisks). D, dorsal; A, anterior; L, lateral; nt, neural tube. (E–G) Transverse sections (labeled with pSMAD1/5/8 antibody [red] and Hoechst stain [blue]) showing that pSMAD1/5/8 is expressed in the dorsolateral otocyst (asterisks; HH 16: n = 9; HH 18: n = 10; HH 20: n = 7), in contrast to *Smad6*, during HH 16–20. D, dorsal; L, lateral; nt, neural tube; ed, endolymphatic duct.

NIH-PA Author Manuscript

NIH-PA Author Manuscript

NIH-PA Author Manuscript

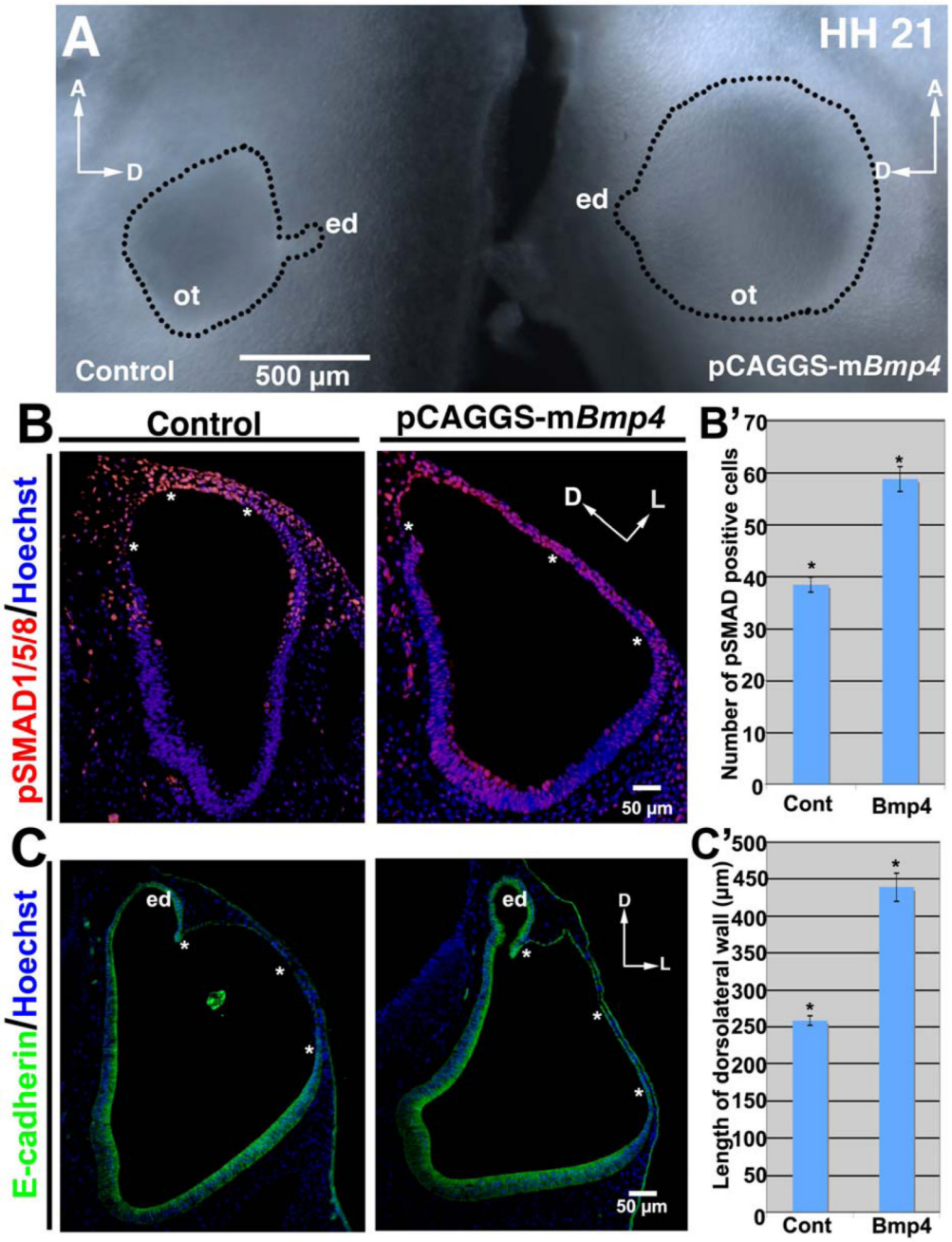

Figure 4. BMP signaling is sufficient to drive rapid thinning and expansion in the chick dorsolateral otocyst

(A) Over expression of *Bmp4* results in formation of an enlarged (hyperexpanded) otocyst (ot) (right side of figure), as compared to the control otocyst (left side of figure), as shown in whole mounts at HH 21. The wall of the otocyst is outlined, along with the endolymphatic duct (ed). A, anterior; D, dorsal; ed, endolymphatic duct. (B, C) Transverse sections (HH 20; B, labeled with pSMAD1/5/8 antibody [red] and Hoechst stain [blue]; C, labeled with E-cadherin antibody [green] and Hoechst stain [blue]) show that *Bmp4* over expression results in an increase in the extent of the dorsolateral otocyst that expresses pSMAD1/5/8 (B; asterisks) as well as an enlargement of the area undergoing rapid thinning and expansion (C;

NIH-PA Author Manuscript

NIH-PA Author Manuscript

NIH-PA Author Manuscript

asterisks). D, dorsal; L, lateral; ed, endolymphatic duct. (B') Graph showing the mean number of pSMAD1/5/8-positive cells (plus/minus standard error of the mean) in the dorsolateral (thinned) region in control (Cont) otocysts, and in otocysts subjected to *Bmp4* over expression (4–5 sections through the mid-anteroposterior extent of the otocyst in 3 control and 3 experimental embryos were counted). *$P < 0.05$ (Student's T-test). (C') Graph showing the mean length (in the mediolateral plane) (plus/minus standard standard error of the mean) of the dorsolateral (thinned) region in control (Cont) otocysts, and in otocysts subjected to *Bmp4* over expression (3 control and 3 experimental embryos were counted, and the thinned region from 4–5 sections of individual embryos were measured). *$P < 0.05$ (Student's T-test).

NIH-PA Author Manuscript

NIH-PA Author Manuscript

NIH-PA Author Manuscript

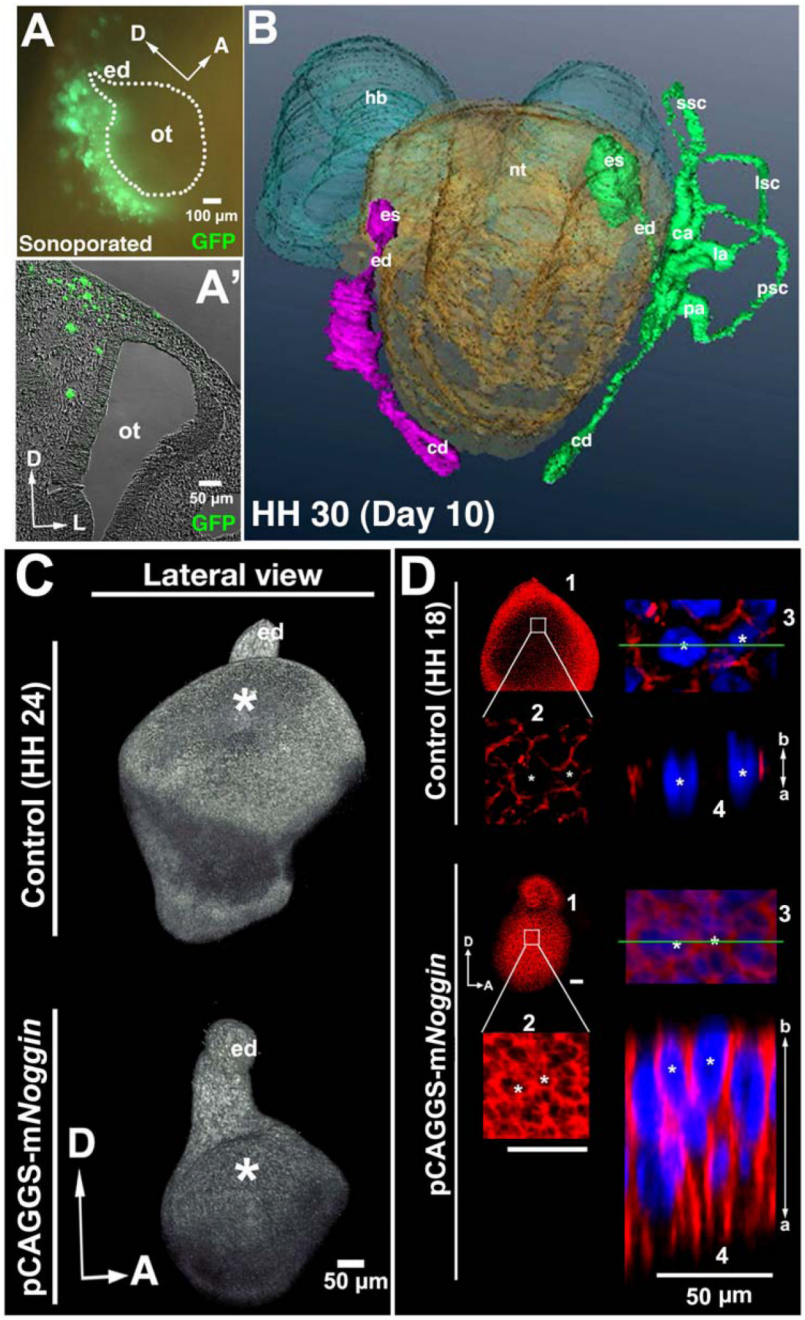

Figure 5. BMP signaling is required for formation of the chick vestibular chamber and for rapid thinning and expansion of the dorsolateral otocyst during formation of the primordial canal outgrowth

(A, A') Whole mount (A) and transverse section (A'; unstained) showing GFP-expressing cells (green) in the mesenchyme posterior to the otocyst 12 hours after sonoporation. The otocyst (ot) and endolymphatic duct (ed) are outlined in A. D, dorsal; A, anterior; L, lateral. (B) Reconstruction showing that at HH 30 (10 days of incubation) the semicircular canals (ssc, lsc, psc), but not the cochlear duct (cd), endolymphatic duct (ed), and endolymphatic sac (es; present but truncated), are absent on the side of the embryo (left side of figure) in which *Noggin* was over expressed (inner ear structures are shown in purple on the *Noggin*-

NIH-PA Author Manuscript

NIH-PA Author Manuscript

NIH-PA Author Manuscript

over expression side; and in green on the control side). ca, cristae ampullaris; la, ampulla of the lateral semicircular canal, pa, ampulla of the posterior semicircular canal. (C) Confocal reconstructions of HH 24 otocysts labeled with E-cadherin showing that expansion of the dorsolateral otocyst is severely attenuated 3 days after sonoporation of the *Noggin* vector (bottom image), as compared to control otocysts (top image). Asterisks mark the dorsolateral otocyst, which has undergone normal expansion in the control otocyst but not in the experimental otocyst, whereas outgrowth of the ventral otocyst and endolymphatic duct (ed) is not affected by *Noggin* over expression. D, dorsal; A, anterior. (D) Confocal imaging showing that in otocysts subjected to *Noggin* over expression, dorsolateral cells remain as elongated pseudostratified columnar epithelial cells, and E-cadherin (red; Hoechst staining of cell nuclei, blue) remains broadly expressed along the apicobasal (a, b) surface of these cells, in contrast to control embryos in which dorsolateral cells become cuboidal to squamous and E-cadherin expression becomes fragmented. D, dorsal; A, anterior. 1, panel showing the entire otocyst. 2, boxed area in panel 1 enlarged. 3, area in panel 2 containing two cells marked with asterisks enlarged. 4, panel showing a lateral view of the epithelium at the level of the green line in panel 3.

NIH-PA Author Manuscript

NIH-PA Author Manuscript

NIH-PA Author Manuscript

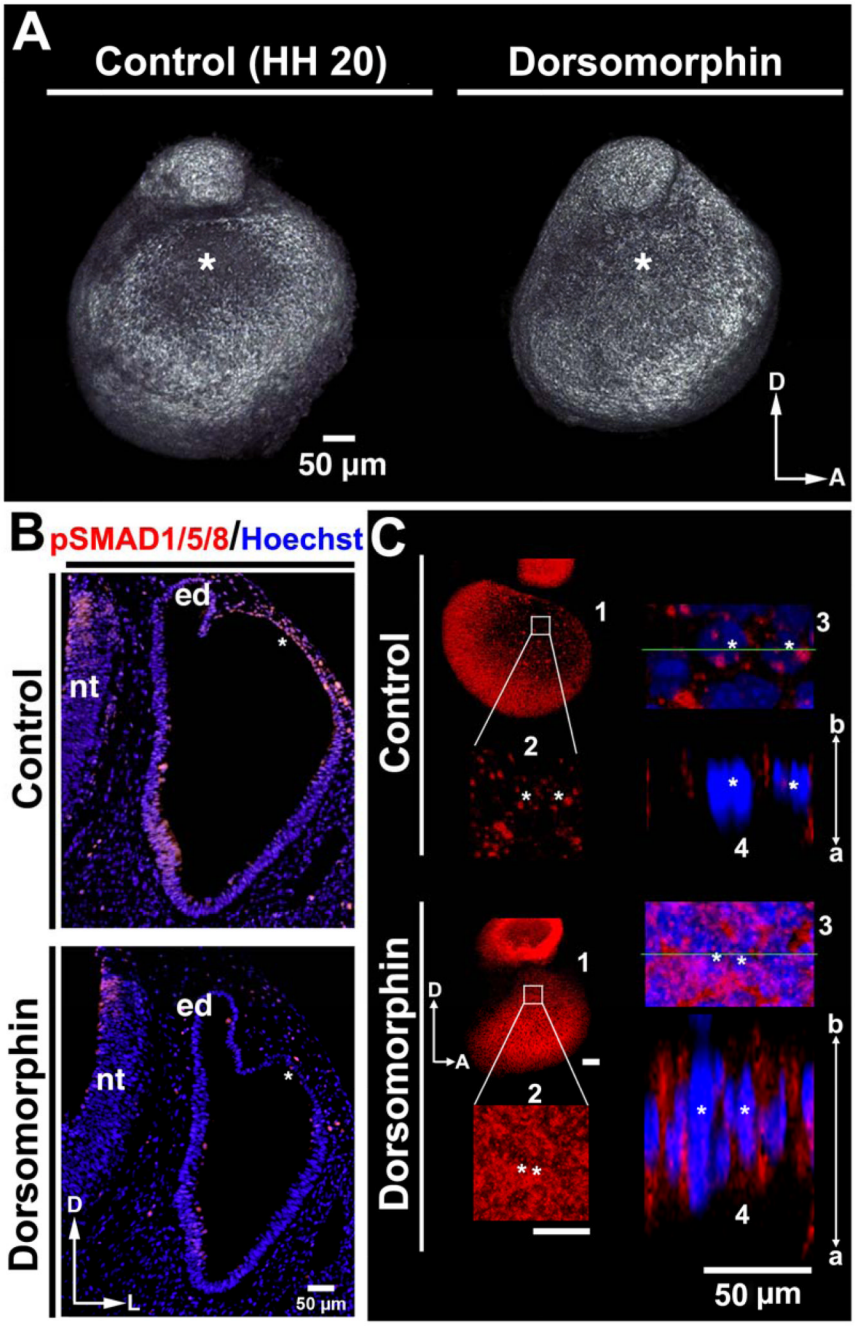

Figure 6. BMP/SMAD signaling is required for rapid thinning and expansion of the chick dorsolateral otocyst

(A) Treatment of embryos with Dorsomorphin results in the formation of slightly smaller otocysts, as compared to those of the controls, as viewed in confocal reconstructions of otocysts labeled with E-cadherin at HH 20. D, dorsal; A, anterior. The asterisks mark the dorsolateral otocyst, which undergoes normal expansion in the control otocyst, but not in the experimental. (B) Transverse sections (HH 20; labeled with pSMAD1/5/8 antibody [red] and Hoechst stain [blue]) after Dorsomorphin treatment show that pSMAD1/5/8 expression occurs in the control dorsolateral otocyst but not in the experimental dorsolateral otocyst (these regions are marked with asterisks). D, dorsal; A, anterior; nt, neural tube; ed,

NIH-PA Author Manuscript

NIH-PA Author Manuscript

NIH-PA Author Manuscript

endolymphatic duct. (C) Confocal imaging showing that the dorsolateral otocysts of Dorsomorphin-treated embryos display an apically-basally broad E-cadherin (red; Hoechst staining of nuclei, blue) distribution similar to that of the normal dorsolateral otocyst cells at stages prior to epithelial thinning and expansion (i.e., at HH 16), whereas control otocysts show fragmented E-cadherin. D, dorsal; A, anterior; a, apical; b, basal. 1, panel showing the entire otocyst. 2, boxed area in panel 1 enlarged. 3, area in panel 2 containing two cells marked with asterisks enlarged. 4, panel showing a lateral view of the epithelium at the level of the green line in panel 3.

NIH-PA Author Manuscript

NIH-PA Author Manuscript

NIH-PA Author Manuscript

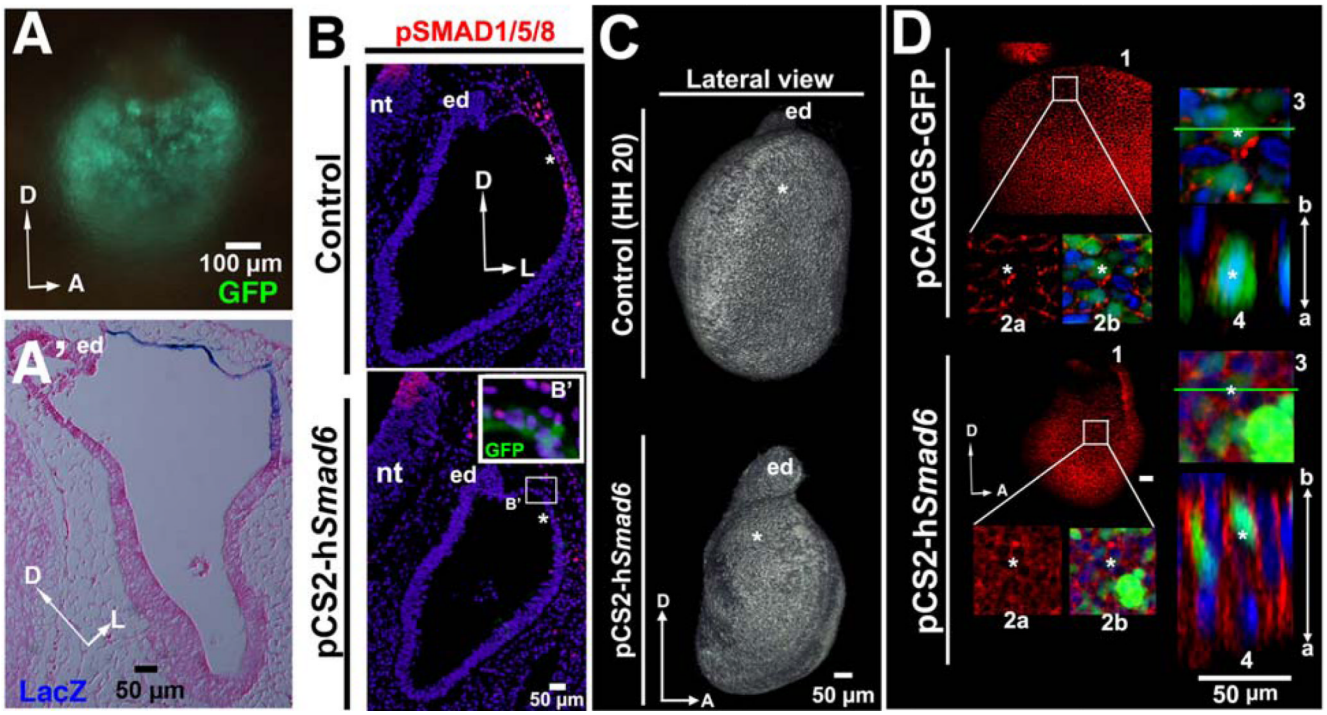

Figure 7. Over expression of *Smad6*, an inhibitor of BMP signaling, inhibits rapid thinning and expansion of the chick dorsolateral otocyst

(A, A') Whole mount and transverse section of the otocyst after its electroporation with both GFP- and LacZ-expressing vectors (GFP: 10–12 hours after electroporation; LacZ: 24 hours after electroporation). The section (HH 20; counterstained with eosin) shows that vector-derived gene expression is restricted to the dorsolateral otocyst (blue staining). D, dorsal; A, anterior; L, lateral; en, endolymphatic duct. (B) Transverse sections (HH 20; labeled with pSMAD1/5/8 and Hoechst stain) showing that the number of pSMAD1/5/8-positive cells is decreased in the dorsolateral otocyst (asterisks) by 24 hours after *Smad6* over expression, but not in the control. D, dorsal; L, lateral; nt, neural tube. (B') Enlargement of the boxed region of the otocyst in which *Smad6* was over expressed, showing that pSMAD1/5/8 labeling (red) is abolished only in transfected cells (green). (C) Confocal reconstructions of otocysts labeled with E-cadherin at HH 20 showing that *Smad6* over expression results in hypoplastic otocysts that fail to undergo expansion of their dorsolateral region (asterisks), as compared to control otocysts. D, dorsal; A, anterior; ed, endolymphatic duct. (D) Confocal imaging showing that E-cadherin (red; cell nuclei stained with Hoechst, blue; GFP, green, indicating transfected cells) is broadly expressed along the apicobasal (a–b) axis of the dorsolateral epithelium of the otocyst in which *Smad6* was expressed, rather than being expressed in a fragmented pattern as in control otocysts in which GFP was ectopically expressed. D, dorsal; A, anterior, a, apical; b, basal. 1, panel showing the entire otocyst. 2, boxed area in panel 1 enlarged. 2a shows only the red (E-cadherin) channel; 2b shows the green (GFP, indicating transfected cells) and blue (Hoechst stained nuclei) as well. 3, area in panel 2 containing two cells marked with asterisks enlarged. 4, panel showing a lateral view of the epithelium at the level of the green line in panel 3.